AIP | Applied Physics Letters

Observation of orientation-dependent photovoltaic behaviors in aligned organic nanowires

Joon Hak Oh, Lydia Helena Wong, Hojeong Yu, Young Jun Park, Jong Min Kim et al.

Citation: Appl. Phys. Lett. **103**, 053304 (2013); doi: 10.1063/1.4817299
View online: http://dx.doi.org/10.1063/1.4817299
View Table of Contents: http://apl.aip.org/resource/1/APPLAB/v103/i5
Published by the AIP Publishing LLC.

Observation of orientation-dependent photovoltaic behaviors in aligned organic nanowires

Joon Hak Oh,[1,2,a)] Lydia Helena Wong,[1,3] Hojeong Yu,[2] Young Jun Park,[4] Jong Min Kim,[4,b)] and Zhenan Bao[1,a)]
[1]*Department of Chemical Engineering, Stanford University, Stanford, California 94305, USA*
[2]*School of Nano-Bioscience and Chemical Engineering, KIER-UNIST Advanced Center for Energy, Low Dimensional Carbon Materials Center, Ulsan National Institute of Science and Technology (UNIST), Ulsan 689-798, South Korea*
[3]*School of Materials Science and Engineering, Nanyang Technological University, Singapore*
[4]*Samsung Advanced Institute of Technology, Samsung Electronics, Yongin 446-712, South Korea*

(Received 7 June 2013; accepted 13 July 2013; published online 1 August 2013)

We fabricated organic nanowire (NW) solar cells based on aligned NWs of *n*-channel organic semiconductor, *N*,*N*′-bis(2-phenylethyl)-perylene-3,4:9,10-tetracarboxylic diimide *via* a filtration-and-transfer alignment method. It is well known that most efficient charge transport typically takes place along the long axis of organic NWs. However, there is no systematic study on the correlation between the orientation of NWs in the active layer and the power conversion efficiency (PCE) of solar cells. Our results demonstrate the effects of alignment direction of NWs on the PCE of organic solar cells with single-crystalline NWs. © *2013 AIP Publishing LLC*. [http://dx.doi.org/10.1063/1.4817299]

Photovoltaic cells made of organic materials have attracted tremendous attention during the last years due to their potential for low-cost, large area, and flexible devices.[1–6] In organic semiconductors, electron-hole pairs, called excitons, are generated upon illumination. These excitons must migrate to a donor-acceptor (D-A) interface where there is an adequate energy drop to induce the exciton dissociation to separate into hole and electron charge carriers. These charge carriers are then transported through the active layer to the corresponding contact. Therefore, exciton diffusion length (L_D) and charge carrier mobility in organic semiconductors are among the key fundamental parameters that affect the power conversion efficiency (PCE). Since most organic semiconductors have a short exciton diffusion length on the order of 5–10 nm, nanostructuring the donor and acceptor phases using the bulk heterojunction (BHJ) structure is of importance for realizing highly efficient organic solar cells.[1,6] However, it remains a challenge to prepare a stable two-phase, nanoscale, and bicontinuous D-A morphology.

Single-crystalline or highly crystalline organic/polymer nanowires (NWs) theoretically have higher charge carrier mobilities and longer exciton diffusion length than their amorphous or polycrystalline thin-film counterparts, owing to their long-range order and high degree of structural perfection.[7,8] Lunt *et al*. demonstrated that the exciton diffusion length in 3,4:9,10-perylenetetracarboxylic dianhydride (PTCDA) is a monotonic function of the extent of crystalline order in the thin films, as in the case of charge carrier mobility.[9] The nanoscale dimension of organic NWs can also be selectively tuned to match the exciton diffusion length. When mixed with the corresponding donor or acceptor, a stable BHJ structure can be readily formed with organic NWs. Several groups have demonstrated the use of organic NWs for organic solar cells. For example, the nanoscale morphologies of poly(3-hexylthiophene) (P3HT)/fullerene blend photovoltaic cells were controlled to achieve higher PCEs using prefiltered P3HT nanofibers,[10] a mixed solvent to tune the crystallinity of P3HT phase,[11,12] or an ultrasonic-assisted nanodimensional self-assembly.[13] Xin *et al*. prepared poly(3-butylthiophene) (P3BT) NWs and observed an order of magnitude increase in PCE from NW photovoltaic cells using fullerene derivatives as the acceptors compared to those of as-cast devices.[14–16] An organogel/polymer system was utilized to fabricate nanostructured BHJ solar cells.[17] Furthermore, organic solar power wires,[18] P3HT/PCBM composite NW solar cells,[19] and self-assembled thiophene derivatives/ZnO hybrid single NW solar cells[20] were reported.

The aforementioned demonstrations clearly showed the great promise of organic NWs for BHJ solar cells. However, the NWs used in those studies were randomly oriented, or a single NW was examined. Ordered nanostructures composed of aligned NWs are envisioned to offer various advantages, such as efficient exciton dissociation *via* denser packing of NWs, less aggregation, higher degree of percolation, and enhanced current output.[21–26] Furthermore, most organic semiconducting NWs for solar cells were prepared from donor materials,[13,16,22,23,26–29] and only few acceptor NWs were reported.[17,24,25] The high absorption coefficient of acceptor NWs at a longer wavelength may afford a high degree of photon absorption.

We previously developed a filtration-and-transfer (FAT) alignment method that allows the efficient alignment of organic wires with controllable densities and the formation of multiple, discrete NW patterns aligned in different directions.[7] The ability to align organic NWs at a high density enabled high and uniform on-currents from organic

[a)]Authors to whom correspondence should be addressed. Electronic addresses: joonhoh@unist.ac.kr and zbao@stanford.edu.
[b)]Present address: Department of Engineering Science, University of Oxford, Parks Road, Oxford OX1 3PJ, United Kingdom.

NW-based transistors. Herein, we report the demonstration of organic photovoltaic devices using ordered single crystalline *n*-channel organic NWs aligned with the FAT alignment method. Although anisotropy of charge carrier mobility in single-crystal organic field-effect transistors (OFETs) along the different crystallographic axes has been demonstrated,[30,31] such anisotropic effects on PCE in organic solar cells have not been reported. We observed the anisotropic photovoltaic behaviors in NW solar cells using aligned *n*-channel NWs with different orientations relative to current flow direction in the photoactive layer.

N,*N*′-bis(2-phenylethyl)-perylene-3,4:9,10-tetracarboxylic diimide (BPE-PTCDI) was used as the acceptor material due to its promising usage in thin-film based organic solar cells,[32] high charge carrier mobilities, strong absorption in the long wavelength ranges, high exciton diffusion length, and its readiness in forming NWs.[7,33] P3HT was employed as the donor material. The chemical structures and energy diagrams of P3HT and BPE-PTCDI are presented in Figure 1(a). The BPE-PTCDI NWs were synthesized using a solvent-exchange method (rapid solution dispersion), where a small amount of concentrated solution was added to an excess (thirty-fold by volume) of poor solvent with vigorous mixing. BPE-PTCDI NWs with an average diameter of about 50 nm were synthesized (Figure 1(b)). The inset of Figure 1(b) exhibits an optical microscope image of BPE-PTCDI NWs aligned with the FAT method.

UV-vis spectra of pure P3HT, pure BPE-PTCDI NW, and P3HT/BPE-PTCDI NW blend film (3/1 by wt. %) are shown in Figure 1(c). For the blend film, a P3HT/BPE-PTCDI NW blend composition of 3/1 was chosen, because it gave the best performance among three different P3HT/BPE-PTCDI NW blend compositions (3/1, 1/1, 1/3 by wt. %) tested. P3HT absorbs up to 630 nm, whereas BPE-PTCDI NW absorbs up to ~750 nm with the maximum absorption at 640 nm. The absorption spectrum of P3HT/BPE-PTCDI blend exhibits a superposition of the individual absorption spectra. This indicates that charge-transfer almost does not take place in the ground state.[17] The photoluminescence (PL) of P3HT/BPE-PTCDI NW blend film was significantly quenched compared to that of pure P3HT (Figure 1(d)), revealing that an efficient charge separation occurred at the P3HT/BPE-PTCDI interface.

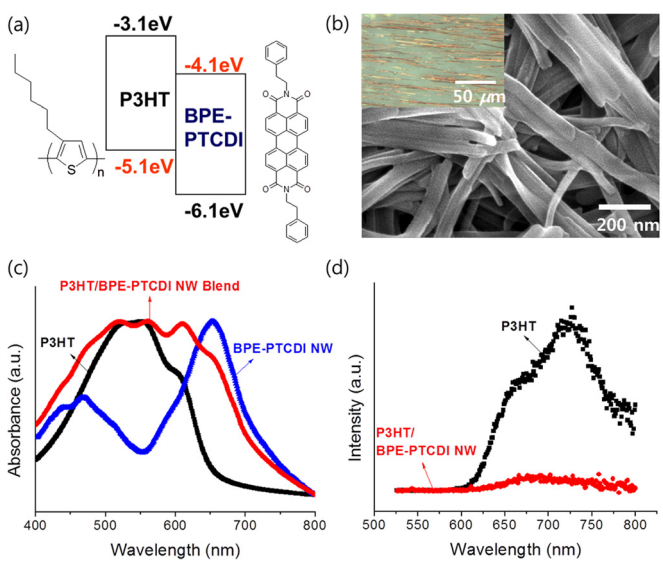

FIG. 1. (a) Chemical structures and energy diagram for P3HT and BPE-PTCDI. (b) SEM image of BPE-PTCDI NWs. (inset) Optical microscope image of aligned BPE-PTCDI NWs. (c) UV-vis spectra of P3HT, BPE-PTCDI NW, and P3HT/BPE-PTCDI NW blend film (3/1 by wt. %), and (d) PL spectra of P3HT and P3HT/BPE-PTCDI NW blend film (3/1 by wt. %). Note that the energy levels for BPE-PTCDI are depicted for solution state. The HOMO and LUMO levels of BPE-PTCDI NW are −6.0 eV and −4.4 eV, respectively.

The schematic illustrations of the device structures are presented in Figure 2. Four different device structures were prepared: (D1) P3HT/thermally evaporated BPE-PTCDI bilayer thin film as a reference for NW structures (Fig. 2(a)), (D2) non-aligned randomly oriented NW BHJ cells (Fig. 2(b)), (D3) P3HT/aligned *n*-channel NW bilayer with lateral electrodes that exhibits charge transport along the diameter of the NW (Fig. 2(c)), and (D4) P3HT/aligned *n*-channel NW bilayer solar cells having electrodes with the photoactive channel width direction perpendicular to the aligned NW, where the current flow path is parallel to the NW alignment direction (an inverted cell structure) (Fig. 2(d)). For the photovoltaic devices with aligned NWs (i.e., D3 and D4), the alignment of NWs was performed using the FAT method, where the filtration power is used as a torque to orient NWs parallel to the long axis of the open stripe pattern of polydimethylsiloxane (PDMS) mask.[7] A densely packed, aligned, monolayer-thick NW pattern prepared using the same PDMS mask and the same concentration of NW solution was utilized as the acceptor material for devices D3 and D4, in order to rule out the effects of the number and density of the NWs. The photoactive area of the devices was defined by the deposited area of Al electrode for devices D1, D2, and D3, while that of device D4 was defined as the light absorbing net area between two electrodes.

The PCEs of the NW solar cells were compared with those of P3HT/thermally evaporated BPE-PTCDI bilayer solar cells, and the large molar absorptivity of BPE-PTCDI is considered to minimize light scattering effect in these NW devices.[34] Bathocuproine (BCP) was used as the exciton blocking layer (EBL). BCP is known to facilitate electron transport from the adjacent acceptor layer to the cathode by establishing an Ohmic contact while blocking excitons in the lower band gap acceptor layer from recombining at the cathode.[35,36] In addition, a BCP buffer layer assists in planarizing the curvature of the underlying BPE-PTCDI NWs.

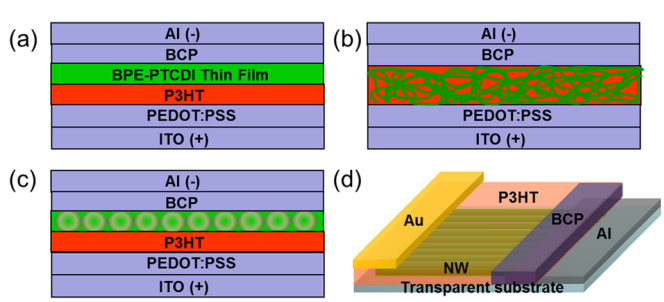

FIG. 2. Device structures tested in this study: (a) P3HT/thermally evaporated BPE-PTCDI bilayer solar cell. (b) P3HT/BPE-PTCDI NW BHJ solar cell. (c) Bilayer NW solar cell with aligned NW. (d) Aligned NW solar cells with electrodes perpendicular to the aligned NW.

Figure 3(a) shows the optimized current density-voltage (J versus V) characteristics of photovoltaic devices under simulated 100 mW cm^{-2} AM 1.5G illumination. The optimized photovoltaic properties of the devices with different structures together with the average PCEs are summarized in Table I. The average PCEs of devices D1, D2, D3, and D4 were 2.18×10^{-3}%, 2.87×10^{-3}%, 3.46×10^{-3}%, and 3.55×10^{-2}%, respectively. P3HT/thermally evaporated BPE-PTCDI bilayer thin film devices (D1) exhibited an optimized PCE of 2.75×10^{-3}%. It should be mentioned that BPE-PTCDI was thoroughly purified three times with sublimation, prior to the thermal evaporation. A similar PCE ($\sim 2 \times 10^{-3}$%) was also observed from CuPc/purified BPE-PTCDI bilayer thin film devices.[32] The comparatively poor

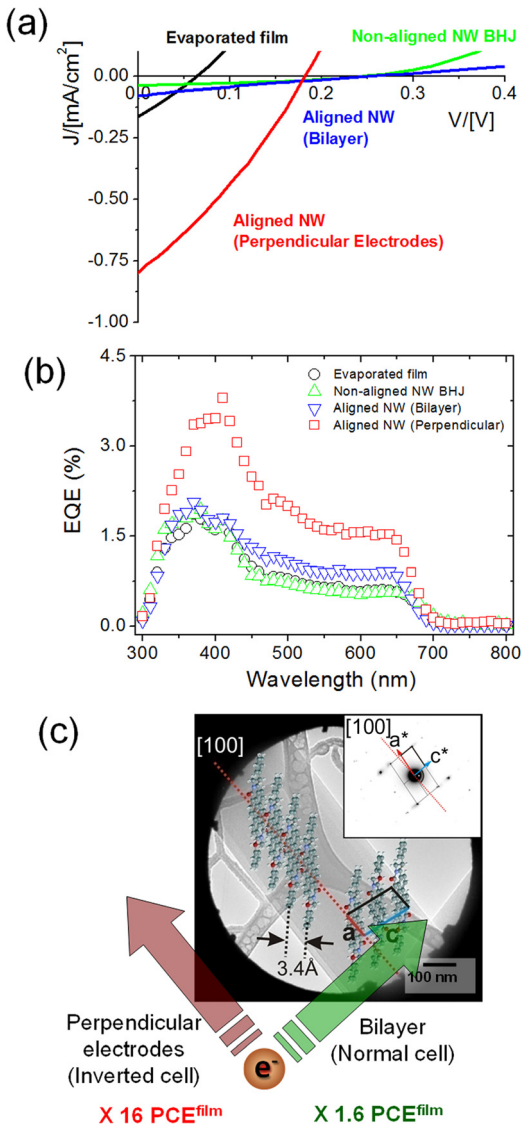

FIG. 3. (a) Current density-voltage (J versus V) curves of photovoltaic devices under white light (the AM 1.5G illumination). (b) EQE of photovoltaic devices constructed using different structures. (c) A TEM image with a selected area aperture of a single BPE-PTCDI MW. (inset) The corresponding SAED pattern (Ref. 7). BPE-PTCDI molecules have a slipped π-stacking structure along the long axis (the a-axis) of the MW with the shortest π-planar distance of 3.4 Å. The aligned NW solar cells with perpendicular electrodes exhibit 16 times higher efficiency compared to that of P3HT/thermally evaporated BPE-PTCDI bilayer thin film devices, whereas bilayer solar cells with aligned NWs as the acceptor layer show 1.6 times higher efficiency.

V_{oc} in P3HT/thermally evaporated BPE-PTCDI bilayer thin film devices (D1) resulted from about one order of magnitude smaller shunt resistance (R_{SH}) value compared with those of NW devices. P3HT/NW BHJ system (D2) gave an optimized PCE of 3.44×10^{-3}% with a V_{oc} of 0.25 V, a J_{sc} of -0.038 mA cm^{-2}, and a FF of 0.37. Through the alignment of NWs, a slightly increased PCE of 4.44×10^{-3}% with a V_{oc} of 0.26 V, a J_{sc} of -0.079 mA cm^{-2}, and a FF of 0.22 was achieved from P3HT/aligned NW bilayer with out-of-plane facing electrodes system (D3). At a given applied voltage, photocurrent J_{ph} is proportional to incident light intensity I, with a relation of $J_{ph} \propto I^{\alpha}$, where $\alpha = 1$ when monomolecular recombination is dominant or when all carriers are swept out prior to recombination.[37,38] On the other hand, α becomes less than 1, due to bimolecular recombination, space charge effects, variations in mobility between the two carriers, or variations in the continuous distribution in the density of states.[37,38] The solar cell devices based on P3HT/BPE-PTCDI film (D1) showed $\alpha = 0.90$ at V = 0 V, which indicates bimolecular recombination effect is relatively low. In contrast, solar cells based on P3HT/randomly oriented NWs BHJ (D2) and aligned NWs/P3HT bilayer (D3) showed α close to 0.5 (0.59 for D2 and 0.51 for D3), indicating the higher possibility of bimolecular recombination. Nonetheless, NW-based devices D2 and D3 exhibited higher PCEs compared with thin-film-based device D1, mainly due to the larger V_{oc}. Despite the low PCE for BPE-PTCDI based solar cells, in general, an important finding in this work is that these NW-based solar cells exhibited relatively higher PCEs than that of P3HT/thermally evaporated BPE-PTCDI bilayer thin film devices (PCE^{film}). This may also be attributed to the single-crystalline defect-free nature of the nanoscale acceptor domains in the NW system.

Very interestingly, a significant enhancement in J_{sc} was clearly observed from the inverted cell device with perpendicular electrodes. The increased photocurrent is attributed to the most efficient charge transport along the long axis direction of the NW with perpendicular electrode system. Combined with its open circuit voltage (V_{oc}) of 0.18 V and fill factor (FF) of 0.30, an optimized PCE of 4.32×10^{-2}% was achieved. This is 16 times higher than PCE^{film}. The relatively lower PCEs of the devices based on P3HT/NW BHJ and P3HT/aligned NW bilayer are predominantly due to the lower J_{sc} values with unfavorable charge transport pathway, while their V_{oc} values are higher than those of other devices. These results substantiate the importance of optimizing charge transport direction for enhancing solar cell performance.

To further confirm the accuracy of the measurements, the external quantum efficiency (EQE) of the devices constructed using different structures or electrode configurations was measured (Figure 3(b)). The observed J_{sc} values are in agreement with the value of J_{sc} obtained from integrating the EQE spectra of the photovoltaic devices. The EQE of the aligned NW solar cells with perpendicular electrodes showed relatively higher photoconversion efficiency in the range of 400–700 nm with the maximum EQE value of 3.8% at 410 nm, compared to those of the other photovoltaic devices. This result agrees well with improvement of the J_{sc} and PCE of the aligned NW device with perpendicular electrodes.

TABLE I. Performance comparison of photovoltaic devices constructed using different structures.

Device type	*n*-Channel semiconductor condition	J_{sc}[a] (mA cm^{-2})	V_{oc}[a] (V)	*FF*[a]	PCE[a] (%)	PCE[aveb] (%)	Remark[c]
D1	Evaporated film	−0.163	0.065	0.26	2.75×10^{-3}	$2.18 (\pm 0.37) \times 10^{-3}$	Reference cell, PCE[film d]
D2	Non-aligned NW BHJ[e]	−0.038	0.25	0.37	3.44×10^{-3}	$2.87 (\pm 0.53) \times 10^{-3}$	×1.3 times
D3	Aligned NW (bilayer)	−0.079	0.26	0.22	4.44×10^{-3}	$3.46 (\pm 0.92) \times 10^{-3}$	×1.6 times
D4	Aligned NW (perpendicular electrodes)	−0.80	0.18	0.30	4.32×10^{-2}	$3.55 (\pm 0.78) \times 10^{-2}$	×16 times

[a]The optimized photovoltaic characteristics.
[b]The average power conversion efficiency with the standard deviation, which was obtained from more than 14 devices.
[c]Comparison was performed for the optimized performance.
[d]CuPc/BPE-PTCDI thin film bilayer devices also showed a similar PCE of 0.002% for pure BPE-PTCDI film.[32]
[e]Optimized composition for NW BHJ:P3HT/BPE-PTCDI NW = 3/1 by wt. %.

The crystallographic orientation of BPE-PTCDI NW has been previously examined by us with transmission electron microscopy (TEM) image and the corresponding diffraction pattern analysis.[7] A TEM image with a selected area aperture and the corresponding selected area electron diffraction (SAED) pattern (inset) of a BPE-PTCDI NW are shown in Figure 3(c). The diffraction patterns obtained at different locations along the single NW exhibited an equivalent crystal-phase geometry, indicating the single-crystalline nature of the BPE-PTCDI NWs.[7] BPE-PTCDI molecules have a slipped π-stacking structure along the *a*-axis of the NW with the shortest π-planar distance of 3.4 Å, indicating the efficient charge-transport pathway along the long axis of the NW. This explains why the aligned NW solar cells having perpendicular electrodes exhibited 16 times higher PCE compared to that of P3HT/thermally evaporated BPE-PTCDI bilayer thin film devices. On the other hand, charge transport of NW in bilayer system takes place along the *c*-axis (similar to the diameter direction) of the crystalline unit cell, and the device showed 1.6 times higher efficiency compared to that of the evaporated bilayer thin film devices.

In conclusion, we have observed PCE anisotropy in organic solar cells based on aligned organic NWs. P3HT/aligned *n*-channel NW solar cells having perpendicular electrodes (D4) with charge carrier transport along the long axis of the NW exhibited 16 times higher PCE compared with the P3HT/vacuum-deposited BPE-PTCDI thin film bilayer solar cells (D1). This originates from the efficient transport of dissociated charges *via* aligned NW system with their intrinsic properties such as longer exciton diffusion length and higher charge carrier mobility. Interestingly, P3HT/aligned *n*-channel NW bilayer solar cells (D3) also showed about two times higher PCEs compared to the thin film counterparts, because charge transport across the diameter of the single-crystalline NW can also be more effective than that in the thermally evaporated thin film. Our results substantiate the high potential of single-crystalline organic semiconductor NWs for use in organic solar cells. Furthermore, our findings demonstrate the anisotropic performance in organic solar cells based on NW arrays with different orientations relative to the electrodes.

This work was supported by Samsung Electronics Co. J.H.O. acknowledges partial financial support from the National Research Foundation of Korea (NRF) funded by the Korean Government (MEST) (Grant Nos. 2010-0025292 and 2011-0017174) and Global Frontier Research Center for Advanced Soft Electronics (Grant No. 2011-0031628). H.Y. acknowledges financial support from the Global Ph.D. Fellowship funded by National Research Foundation of Korea (NRF).

[1]A. Mayer, S. Scully, B. Hardin, M. Rowell, and M. McGehee, Mater. Today **10**, 28 (2007).
[2]C. J. Brabec, N. S. Sariciftci, and J. C. Hummelen, Adv. Funct. Mater. **11**, 15 (2001).
[3]G. Li, V. Shrotriya, J. S. Huang, Y. Yao, T. Moriarty, K. Emery, and Y. Yang, Nat. Mater. **4**, 864 (2005).
[4]W. L. Ma, C. Y. Yang, X. Gong, K. Lee, and A. J. Heeger, Adv. Funct. Mater. **15**, 1617 (2005).
[5]B. C. Thompson and J. M. Frechet, Angew. Chem., Int. Ed. **47**, 58 (2008).
[6]G. Dennler, M. C. Scharber, and C. J. Brabec, Adv. Mater. **21**, 1323 (2009).
[7]J. H. Oh, H. W. Lee, S. Mannsfeld, R. M. Stoltenberg, E. Jung, Y. W. Jin, J. M. Kim, J.-B. Yoo, and Z. Bao, Proc. Natl. Acad. Sci. U.S.A. **106**, 6065 (2009).
[8]H. Li, G. Giri, J. B.-H. Tok, and Z. Bao, MRS Bull. **38**, 34 (2013).
[9]R. R. Lunt, J. B. Benziger, and S. R. Forrest, Adv. Mater. **22**, 1233 (2010).
[10]S. Berson, R. De Bettignies, S. Bailly, and S. Guillerez, Adv. Funct. Mater. **17**, 1377 (2007).
[11]A. J. Moulé and K. Meerholz, Adv. Mater. **20**, 240 (2008).
[12]T. Salim, L. H. Wong, B. Brauer, R. Kukreja, Y. L. Foo, Z. Bao, and Y. M. Lam, J. Mater. Chem. **21**, 242 (2011).
[13]B. G. Kim, M. S. Kim, and J. Kim, ACS Nano **4**, 2160 (2010).
[14]H. Xin, F. S. Kim, and S. A. Jenekhe, J. Am. Chem. Soc. **130**, 5424 (2008).
[15]H. Xin, G. Q. Ren, F. S. Kim, and S. A. Jenekhe, Chem. Mater. **20**, 6199 (2008).
[16]H. Xin, O. G. Reid, G. Ren, F. S. Kim, D. S. Ginger, and S. A. Jenekhe, ACS Nano **4**, 1861 (2010).
[17]A. Wicklein, S. Ghosh, M. Sommer, F. Wurthner, and M. Thelakkat, ACS Nano **3**, 1107 (2009).
[18]M. R. Lee, R. D. Eckert, K. Forberich, G. Dennler, C. J. Brabec, and R. A. Gaudiana, Science **324**, 232 (2009).
[19]K. Kim, J. W. Lee, S. H. Lee, Y. B. Lee, E. H. Cho, H. S. Noh, S. G. Jo, and J. Joo, Org. Electron. **12**, 1695 (2011).
[20]A. L. Briseno, T. W. Holcombe, A. I. Boukai, E. C. Garnett, S. W. Shelton, J. J. Frechet, and P. Yang, Nano Lett. **10**, 334 (2010).
[21]J. S. Kim, Y. Park, D. Y. Lee, J. H. Lee, J. H. Park, J. K. Kim, and K. Cho, Adv. Funct. Mater. **20**, 540 (2010).
[22]M. Aryal, K. Trivedi, and W. W. Hu, ACS Nano **3**, 3085 (2009).
[23]X. He, F. Gao, G. Tu, D. Hasko, S. Huttner, U. Steiner, N. C. Greenham, R. H. Friend, and W. T. Huck, Nano Lett. **10**, 1302 (2010).
[24]X. He, F. Gao, G. Tu, D. G. Hasko, S. Hüttner, N. C. Greenham, U. Steiner, R. H. Friend, and W. T. S. Huck, Adv. Funct. Mater. **21**, 139 (2011).

[25]C. Y. Chang, C. E. Wu, S. Y. Chen, C. Cui, Y. J. Cheng, C. S. Hsu, Y. L. Wang, and Y. Li, Angew. Chem., Int. Ed. **50**, 9386 (2011).
[26]D. Chen, W. Zhao, and T. P. Russell, ACS Nano **6**, 1479 (2012).
[27]G. Ren, P. T. Wu, and S. A. Jenekhe, ACS Nano **5**, 376 (2011).
[28]A. H. Rice, R. Giridharagopal, S. X. Zheng, F. S. Ohuchi, D. S. Ginger, and C. K. Luscombe, ACS Nano **5**, 3132 (2011).
[29]J. S. Kim, J. H. Lee, J. H. Park, C. Shim, M. Sim, and K. Cho, Adv. Funct. Mater. **21**, 480 (2011).
[30]V. C. Sundar, J. Zaumseil, V. Podzorov, E. Menard, R. L. Willett, T. Someya, M. E. Gershenson, and J. A. Rogers, Science **303**, 1644 (2004).
[31]C. Reese and Z. Bao, Adv. Mater. **19**, 4535 (2007).
[32]A. Liu, S. Zhao, S. B. Rim, J. Wu, M. Konemann, P. Erk, and P. Peumans, Adv. Mater. **20**, 1065 (2008).
[33]H. Yu, Z. Bao, and J. H. Oh, Adv. Funct. Mater. **23**, 629 (2013).
[34]F. Nolde, W. Pisula, S. Muller, C. Kohl, and K. Müllen, Chem. Mater. **18**, 3715 (2006).
[35]P. Peumans and S. R. Forrest, Appl. Phys. Lett. **79**, 126 (2001).
[36]M. Vogel, S. Doka, C. Breyer, M. C. Lux-Steiner, and K. Fostiropoulosa, Appl. Phys. Lett. **89**, 163501 (2006).
[37]L. Liu, W. E. Stanchina, and G. Li, Appl. Phys. Lett. **94**, 233309 (2009).
[38]S. R. Cowan, A. Roy, and A. J. Heeger, Phys. Rev. B **82**, 245207 (2010).